Grant Agreement No. 783169
U-Geohaz – "Geohazard impact assessment for urban areas"

Deliverable D4.9: Preliminary rainfall thresholds for the Canary Island

A deliverable of WP 4 (Activity 4.5): Rainfall thresholds for the possible initiation of rockfalls

Due date of deliverable: 31/08/2018
Actual submission date: 10/09/2018

Lead contractor for this deliverable: IRPI

Dissemination Level		
PU	Public	X
PP	Restricted to other programme participants (including the Commission Services)	
RE	Restricted to a group specified by the Consortium (including the Commission Services)	
CO	Confidential, only for members of the Consortium (including the Commission Services)	
TN	Technical Note, not a deliverable, only internal for members of the Consortium	

European Union
Civil Protection and Humanitarian Aid

Table of Content

EXECUTIVE SUMMARY

The document, which represents the fourth deliverable of WP4 “Tools and methods to support Early Warning System for Rockfalls”, describes the actions performed in the Activity 4.5 “Rainfall thresholds for the possible initiation of rockfalls”. The main goal of this activity is the definition of empirical rainfall thresholds for the possible initiation of rockfalls in the Canary Islands.

The report describes the preliminary empirical cumulated event rainfall – rainfall duration (*ED*) thresholds for the Gran Canaria and Tenerife test sites. For the purpose, an algorithm for the objective and reproducible reconstruction of rainfall events and of rainfall conditions responsible for rockfalls is used. A frequentist statistical method is adopted to define *ED* thresholds for different exceedance probabilities.

REFERENCE DOCUMENTS

N°	Title
RD1	DoW Part B

CONTRIBUTORS

Contributor(s)	Company	Contributor(s)	Company
Silvia Peruccacci	CNR-IRPI	Roberto Sarro	IGME
Stefano Luigi Gariano	CNR-IRPI	Rosa Maria Mateos	IGME
Maria Teresa Brunetti	CNR-IRPI	Gerardo Herrera	IGME
Massimo Melillo	CNR-IRPI	Marta Bejar	IGME
Paola Reichenbach	CNR-IRPI	Miguel Tomé	DGPCE
Ivan Marchesini	CNR-IRPI	Lucrecia Alguacil	DGPCE
Mauro Rossi	CNR-IRPI	Jorge Naranjo	CDCP
		Ada Martín	CDCP

REVIEW: CORE TEAM

Reviewed by	Company	Date	Signature
Oriol Monserrat	CTTC	10/09/2018	

1 INTRODUCTION

Rainfall is a recognized trigger of landslides, and investigators have long attempted to determine the amount of precipitation needed to trigger slope failures. Landslides triggered by rainfall are caused by the build-up of water pressure into the ground (Campbell, 1975; Wilson, 1989). Groundwater conditions responsible for slope failures are related to rainfall through infiltration, soil characteristics, antecedent moisture content, and rainfall history (Wieczorek, 1996). These phenomena are poorly understood, and prediction of rainfall-induced landslides is problematic.

Worldwide, rainfall-induced landslides are recurrent phenomena that cause societal and economic damage. Thus, assessing the rainfall conditions responsible for landslides is important and may contribute to reducing risk.

At regional and global scales, empirical approaches to forecast the occurrence of rainfall-induced landslides rely upon the definition of rainfall thresholds, i.e. the rainfall conditions that when reached or exceeded are likely to result in single or multiple landslides. Several authors have proposed different methods to compute rainfall thresholds through the statistical analysis of empirical distributions of rainfall conditions that have presumably resulted in landslides including cumulated event rainfall vs. rainfall duration or mean rainfall intensity vs. rainfall duration (e.g., Aleotti, 2004; Guzzetti et al., 2007, 2008; Brunetti et al., 2010; Berti et al., 2012; Giannecchini et al., 2012; Martelloni et al., 2012; Peruccacci et al., 2012; Staley et al., 2013; Segoni et al., 2014; Rosi et al., 2016; Peruccacci et al., 2017).

Rainfall thresholds are affected by uncertainties that limit their use in operational warning systems. A source of uncertainty lies in the characterization of the rainfall events responsible for landslides. Objective criteria for the definition of rainfall events are lacking. To overcome the problem, Melillo et al. (2018) have proposed an algorithm that reconstructs rainfall events, identifies the rainfall conditions that have resulted in landslides, and calculates probabilistic cumulated event rainfall- rainfall duration (*ED*) thresholds and their associated uncertainties.

The main goal of WP4 is to tailor tools and methods to generate information useful to support early warning systems for rockfalls. An important element to mitigate landslide hazard and risk is the definition of an operational landslide warning system based on the comparison between rainfall measurements and forecasts and rainfall thresholds, aiming at evaluating the possible occurrence of landslides.

The document is organized as follows. After a description of the general settings of the Canary Islands and of the U-Geohaz two test sites (Section 2), we describe the preliminary catalogue of rainfall events that have caused rockfalls in Tenerife Island and along the GC-200 road (Gran Canaria), and the sources and method used for its compilation (Section 3). Next, we describe the CTRL Tool (CTRL-T) used to determine *ED* rainfall thresholds (Section 4). Finally, we exploit the two catalogues to define preliminary empirical rainfall thresholds for possible rockfall occurrence in GC-200 and Tenerife test sites (Section 5).

2 TEST SITES DESCRIPTION

The Canary Islands is an archipelago of seven major volcanic islands constituting the outermost Spanish region in the Atlantic Ocean on the continental slope and rise of western Africa (Figure 1). The islands lie 2000 km east of the Mid-Atlantic Ridge and 150 km west of Morocco. From east to west, the islands are Lanzarote, Fuerteventura, Gran Canaria, Tenerife, La Gomera, La Palma, and El Hierro. The eruptive history of the islands extend from 40 Ma until the present (El Hierro), making into one of the major volcanic oceanic island groups of the world. Most of the historical eruptions in the Canary Islands have been short-lived basaltic or strombolian eruptions, which have caused pyroclastic cones of different size and lava flows of different extend and height.

The steep topography and geological complexity of the archipelago influence the activation of intense slope dynamics and many slope failures occur along the slopes. Rockfalls are the most frequent and damaging landslide type in the Canary Islands, causing damages on built-up areas and communication networks. To define empirical rainfall thresholds for the possible initiation of rockfalls, two test sites were selected following the emergency services priorities. The first site is located in the northwestern part of Gran Canaria Island, along the GC-200 road between the localities of Agaete and Aldea. The second site is represented by the entire Tenerife Island.

Figure 1. The Canary island archipelago. Empirical rainfall thresholds for the possible initiation of rockfalls were defined in two test sites (red boxes).

2.1 GC-200 road (Gran Canaria Island)

Gran Canaria is the third island in size of the Canary Islands, with an area of 1560 km^2 and a maximum altitude of 1956 m. The origin of the island can be dated about 15 million years ago with the first submarine building stages of the Gran Canaria Volcano. Figure 2 shows a simplified geological map of the island with the main lithological units. The main stages of evolution of Gran Canaria are: i) the shield stage, including a basaltic shield volcano; ii) the vertical caldera collapse, giving place to the Tejeda-Fataga complex, with a salic post-caldera resurgence; and iii) a rejuvenated stage, including the Roque Nublo stratovolcano and the post- Roque Nublo volcanism (late eruptive phase) which created a composite monogenetic volcanic field.

Additionally, massive flank failures are mapped (see gravitational failures) giving place to chaotic deposits that cover large areas.

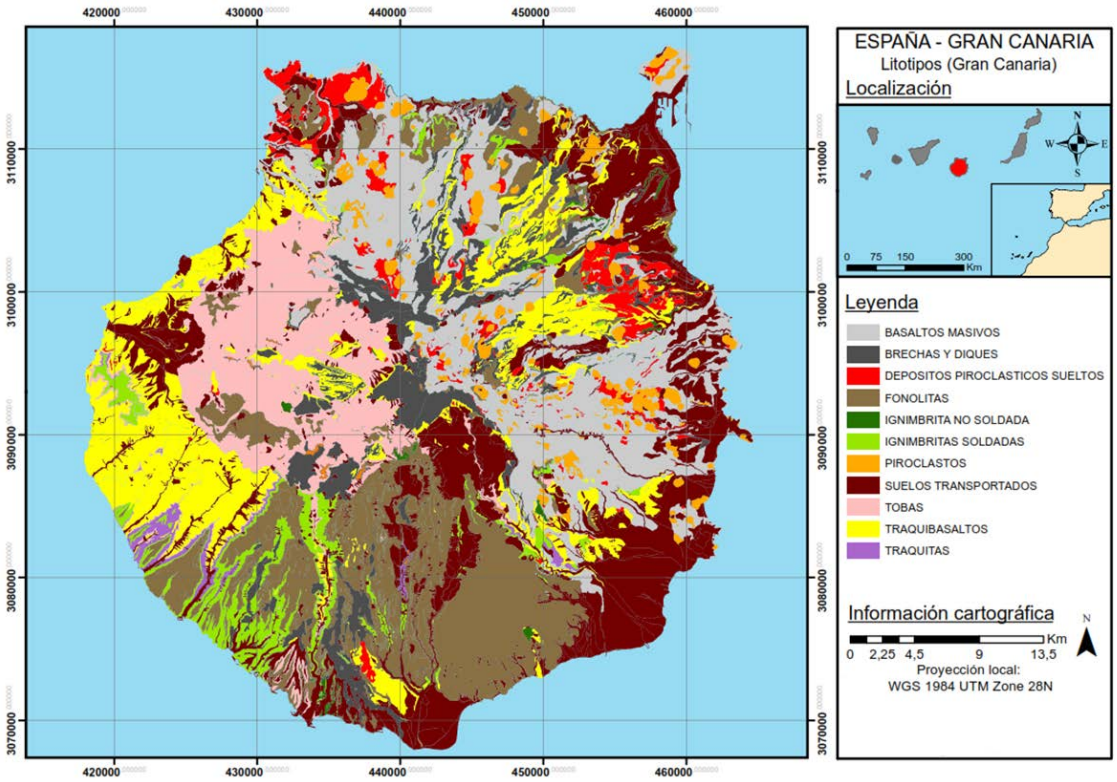

Figure 2. Gran Canaria Island. Simplified geological map.

Regarding climatological conditions, Gran Canaria is located in a transitional zone between temperate and tropical conditions. The conical morphology of Gran Canaria retains the humidity of the predominant north/northeast trade winds of the subtropical Azores anticyclone on the north side of the island. As a result, the northern flanks are humid and vegetation is vigorous, while the south is very dry and the conditions are very arid and desert-like. Rainfall increases with altitude, ranging between less than 200 mm/yr at the coast and over a wide area in southern Gran Canaria, and more than 1400 mm/yr in the higher peaks of the central part of the island. The climate in the test-site area is very dry, with an annual average precipitation of 300 mm and the annual average temperature of 20.6º. The maximum precipitation takes place during the autumn and winter months, with December the rainiest month. Heavy storms are frequent, associated with intense rainfall and strong winds, with events measuring of up to 75 mm in 24 hours.

The GC-200 road test site (Figure 3) is located in the western part of the island, between the localities of Agaete and Aldea, representing the main transportation corridor between the two localities. The road has a length of 34 km, with a very tortuous path following the coastline, a very step coast with the highest cliffs in Europe (Risco Faneque, 1027 m a.s.l.). The road is a strategic infrastructure for the transportation of the tomato production, cultivated in numerous greenhouses in Aldea. Moreover, the road an important touristic attraction due to the spectacular landscape

views. The road has heavy traffic estimated on average with 1500 vehicles per day, with a greater number of vehicles during the period from October to May. The geology of the test-site area is in the domain of the basaltic shield stage, Middle Miocene in age. Along the road, an alternate of alkaline basaltic deposits (hard rocks) and pyroclastic flows can be observed. Both materials can be source areas for rockfalls blocks. In some parts, gravitational deposits also outcrop and some boulders frequently occupy the road.

Figure 3. Gran Canaria Island. Panoramic view of the GC-200 road.

2.2 Tenerife Island

Tenerife is located in the central part of the Archipelago, between 27º 59' 59'' N and 28º 35' 15'' N and 16º 50' 27'' W and 16º 55' 40'' W. It is the largest island with a surface of 2057 km^2 and the most populated. Its highest point, Mount Teide, with an elevation of 3718 meters, is the highest point of Spain and the third largest volcano in the world considering the base at the bottom of the sea.

From the geological point of view, all Canary Islands are located inside the Africa Plate, in the transitional zone between the Continental Crust and the Oceanic Crust, characterized by the volcanic origin that is still active. The tectonic lines are responsible for the island shape– a triangle-, with a clear predominance of NE-SW and NW-SE directions during the main building phases. The principal structures in the Tenerife make the central highlands, with the Teide–Pico Viejo complex and the Las Cañadas areas, the most prominent area with a surface of 130 km^2. Las Cañadas caldera was formed by a vertical collapses produced after intense explosive volcanic activity. The area is partially occupied by the Teide-Pico Viejo strato-volcano and by the volcanic materials derived by different eruptions. The location of Tenerife Island in the middle of the archipelago explains the impressive relief, the large variations of volcanic rocks types and the

different volcanic structures and landforms. The steep orography (Figure 4) of the island and the climate variety have resulted in a diversity of landscapes and geographical formations. The Teide National Park is characterized by extensive pine forests juxtaposed against the volcanic landscape at the summit of Teide and Malpaís de Güímar, to the Acantilados de Los Gigantes (Cliffs of the Giants) with its vertical precipices.

Figure 4. Tenerife Island. Panoramic view of the Anaga range in the northern part of the island.

The trade-winds affect the island during the main part of the year, from May to September. The trade-winds present a double layer, the lower is wet and temperate blowing over the ocean from N-NE direction, the upper layer is warm and very dry blowing from W-NW direction. This layered structure produces a stable situation in the atmosphere. The landforms act as interference with the regional atmosphere circulation producing a wide variety of local climates. North areas are exposed to trade-winds and Atlantic winds, producing the south slopes drier than the north ones; in the northern slopes the presence of the temperature inversion produce a sea cloud, between 500 m to 1500 m high, producing unusual wet conditions and supporting an extra amount of water by fog rain. Several experiments provide evidence for supplies of fog rain four times more than normal rain. During winter, the Atlantic low pressure can descend producing rainy weather and even snow fall above 1500 meters.

3 RAINFALL AND LANDSLIDE DATA

In the test areas, rainfall measurements were obtained from regional rain gauge networks. For the selection of the rain gauge, the available time series, the data quality and the location of the rain gauge were taken into account, given that these points are very crucial to characterize the spatio-temporal variation of the precipitations.

For the Tenerife island test site, we have used the rain gauge network provided by the Spanish National Meteorological Service (AEMET). When the analysis was performed, daily data from the AEMET network were available for the period 2010-2016. As a result, a long time series of rainfall data was obtained, which is an important condition to prepare comprehensive thresholds based on the rainfall analysis. The AEMET network in the Tenerife test site is composed by 66 rain gauges distributed along the island. Among those, 11 rain gauges in the network had no records due to malfunction or other unknown circumstances (Figure 5).

The daily rainfall data were stored in a txt file, in which the header contains information on rain gauge code, rain gauge name, the date (month and year), geographical coordinates, and elevation. In addition, the last 31 rows of the txt file, report information about the daily rainfall in mm. The daily rainfall has referred to the period between 07:00 UTC of the previous day to 07:00 UTC of the day of measurement. This information was stored in a worksheet for the calculation of rainfall thresholds.

As concern the rockfall data, we used the inventory of the Tenerife Island carried out by the Canarian Civil Protection Authorities that registers accurately the location of each rockfall impact along the Tenerife roads. In the period from August 2010 to September 2013, 1860 rockfalls were identified. From the rockfall inventory, we have developed a worksheet to store all data. For each event, the catalogue contains the following information: event code, localization, geographic accuracy, and temporal information of the failure (day, month, year, time, date, temporal accuracy).

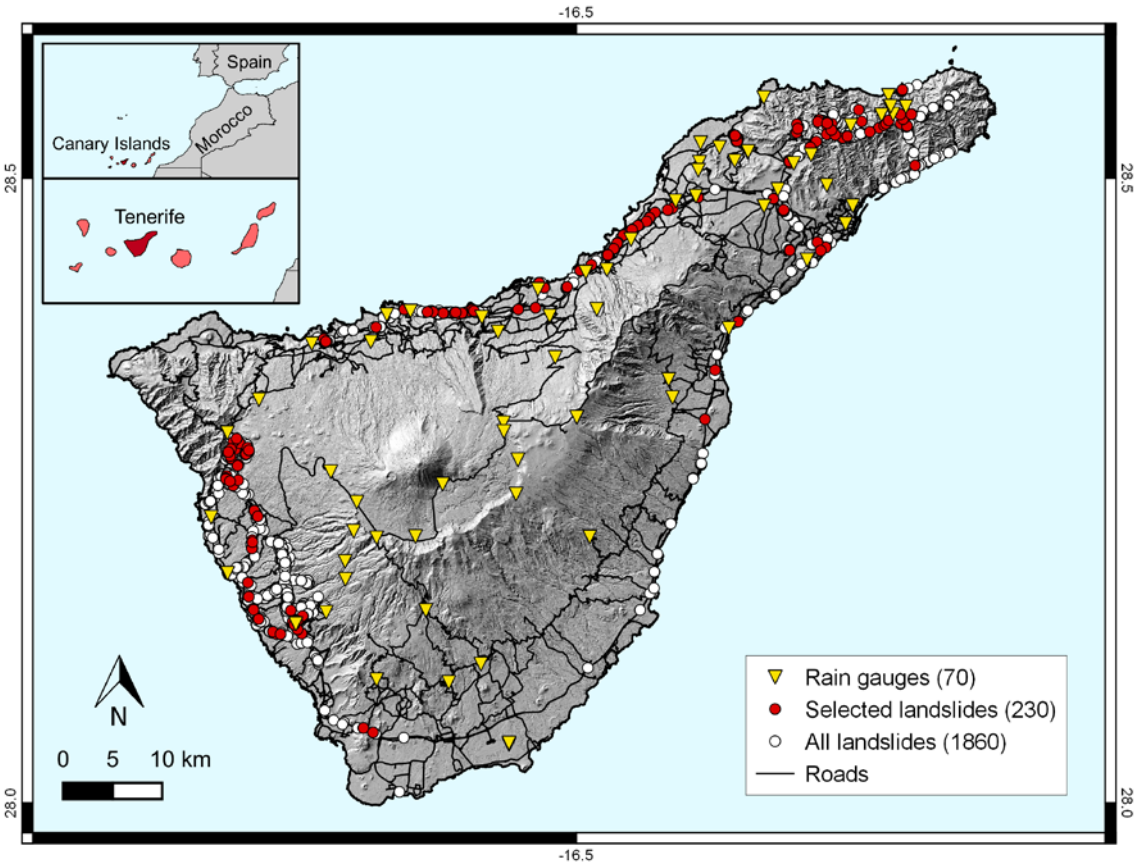

Figure 5. Tenerife Island. Location of the rain gauges (yellow triangles) and rockfalls (red and white circles). White circles show the rockfalls in the catalogue; red circles the events selected to evaluate the threshold.

In the GC-200 test site (Gran Canary), rainfall information available by AEMET were not used because the density and the distribution of the rain gauges over the region were poor. In this case we used for the analysis, data from the Consejo Insular de Aguas rain gauge network, located closest to the rockfall locations (Figure 6). Rainfall data contains daily rainfall measurements collected in the period between January 2010 and December 2017 by a network of 13 rain gauges. Following the same methodology applied in the Tenerife test site, for each rain gauge, data are stored in a worksheet, where the header contains information on rain gauge name, code, geographical coordinates, elevation and the daily rainfall in mm.

We have recorded the information and observations carried out by the Canarian Civil Protecion Autorithies about rockfall events occurred from January 2010 to March 2016, along the GC-200 road. A total of 7811 rockfall events were documented and a digital inventory was prepared defining accurately the location of each impact along the road using orthophotos available for the region. The information for each event includes the kilometre point, number of events, date, boulder size, and was organized in a worksheet. This worksheet contains the following information for each event: event code, localization, geographic accuracy, and temporal information of the failure (day, month, year, time, date, temporal accuracy).

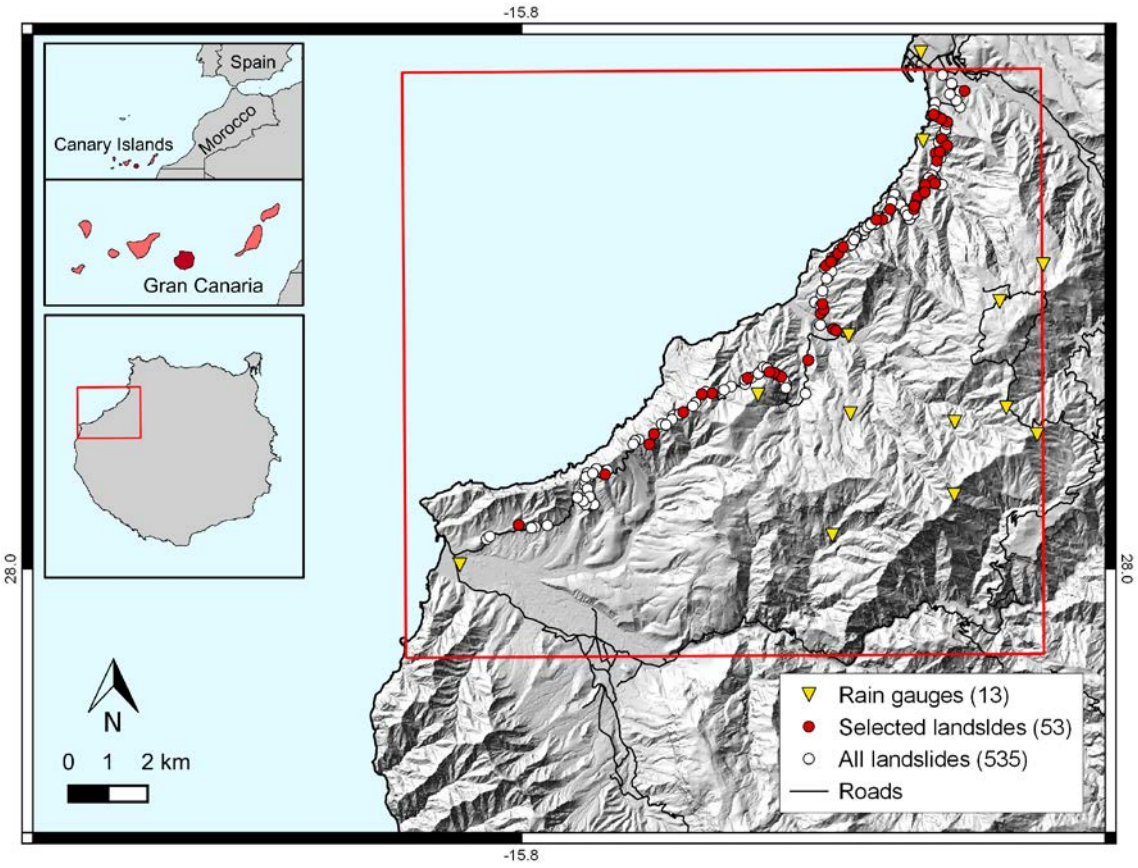

Figure 6. GC-200 test site. Location of the rain gauges (yellow triangles) and rockfalls (red and white circles). White circles show the rockfalls in the catalogue; red circles the events selected to evaluate the threshold.

To reduce the use of wrong information (i.e., incorrectly dated landslides) in the definition of the thresholds, we discarded rainfall conditions showing a delay between the rainfall ending time and the landslide occurrence longer than 48 hours.

In the Tenerife Island, between 2010 and 2016, 230 rockfalls were selected for the analysis (Figure 5), with peaks in 2014 (64 records) and 2012 (45). The monthly distribution is similar to the Gran Canaria, with almost all events recorded between October and April, with a maximum in November (76 records). No landslides were recorded in June and July (Figure 7). The rainfall conditions associated to these failures have durations ranging from 24 to 360 hours and mean value of 53 hours. The values of cumulated rainfall range from 15.4 to 235 mm, with an average of 70.4 mm. The average distance between the landslides and the representative rain gauges is 2.4 km, with a maximum distance of 5 km. More details are reported in Table 1.

The 53 events registered for the Gran Canaria (Figure 6) occurred between 2012 and 2016, most. of them in 2015 (22) and 2016 (16). Almost of the landslides were recorded in the semester October-March, with a peak in February (14 occurrences). Only 7 landslides occurred in the period April-September (Figure 7). The 53 rainfall conditions responsible for the rockfall occurrences have durations in the range $24 \leq D \leq 264$ h (with an average value of 42 h) and cumulated rainfall in the range $16.5 \leq E \leq 219.9$ mm (average value 51.6 mm). All the conditions

were recorded in rain gauges located at a maximum distance from the failures of 5.7 km, with a mean value of 2.8 km. More details are reported in Table 1.

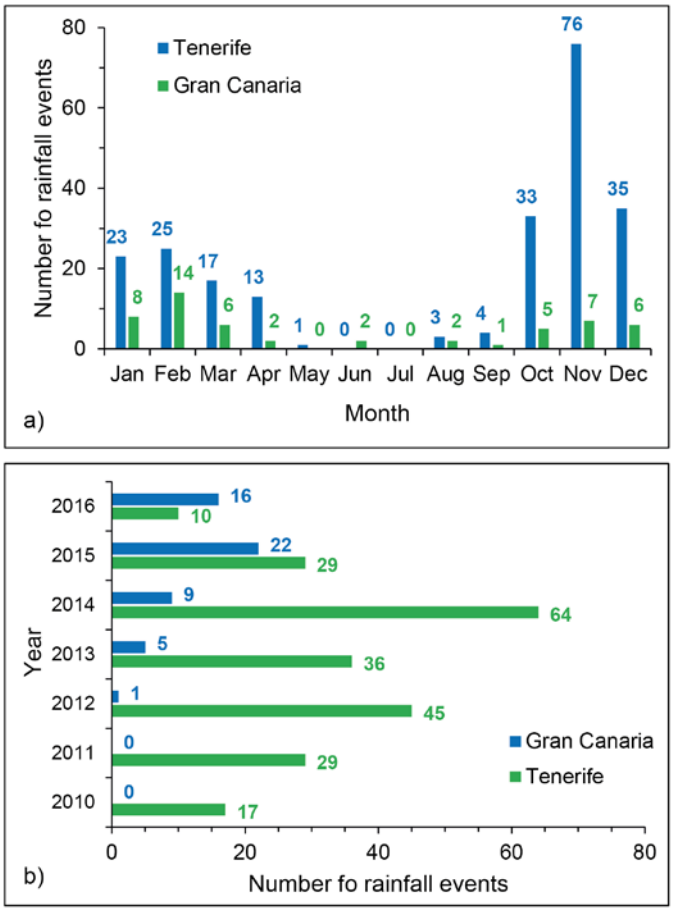

Figure 7. Monthly (a) and annual (b) distributions of the rainfall events reconstructed for the two test sites.

Table 1. Minimum, mean, and maximum values of distance from rain gauge, duration and cumulated event rainfall of the rainfall events reconstructed for the two test sites.

		Rain gauge distance (km)	Duration *D* (h)	Cumulated event rainfall *E* (mm)
Tenerife test site	Min	0.1	24.0	15.4
	Mean	2.4	53.4	70.4
	Max	5.0	360.0	235.0
Gran Canaria test site	Min	0.3	24.0	16.5
	Mean	2.8	41.7	51.6
	Max	5.7	264.0	219.9

4 METHODS

Empirical rainfall thresholds are affected by several uncertainties, including: (i) the availability and quality of the rainfall measurements and of the landslide information; (ii) the characterization of the rainfall event responsible for the landslides; (iii) the heuristic or statistical methods used to determine the thresholds. Standards for measuring landslide-triggering rainfall conditions are still lacking or insufficiently formalized in literature and how the rainfall responsible for the landslide occurrence is calculated is rarely reported. Moreover, the majority of empirical rainfall thresholds available in the literature are calculated using subjective and scarcely repeatable methods.

We maintain that the quantitative identification of the landslide-triggering rainfall and the definition of reliable thresholds are fundamental steps towards a well-founded landslide prediction (Peruccacci et al., 2017; Melillo et al., 2018). The use of a standardized and automatized procedure for the reconstruction of the rainfall conditions responsible for failures and for threshold calculation is necessary for enhancing the objectivity and reproducibility of the thresholds, especially for thresholds to be used in landslide early warning systems. For the purpose, the algorithm CTRL-T proposed by Melillo et al. (2018) was exploited to calculate cumulated event rainfall- rainfall duration (*ED*) thresholds for the Canary Islands.

CTRL-T exploits continuous rainfall measurements, and landslide information, to (1) reconstruct rainfall events; (2) select automatically the representative rain gauges; (3) identify multiple rainfall conditions responsible for the failure in terms of *D* and *E*; (4) attribute a probability to each rainfall condition; and (5) calculate probabilistic rainfall thresholds and their associated uncertainties.

Figure 8 illustrates the logical framework of CTRL-T. The input data is composed by: (i) setting parameters of the rainfall events, (ii) rainfall data, (iii) rain gauge locations, (iv) landslide locations, and (v) landslide occurrence times. The algorithm is divided into three main logical blocks. The “BLOCK 1” executes the reconstruction of the rainfall events (RE). The “BLOCK 2” selects the rainfall events that have resulted in landslides and determines the rainfall duration, D_L, and the cumulated event rainfall, E_L, responsible for the landslides. The “BLOCK 3” calculates rainfall thresholds at different exceedance probabilities.

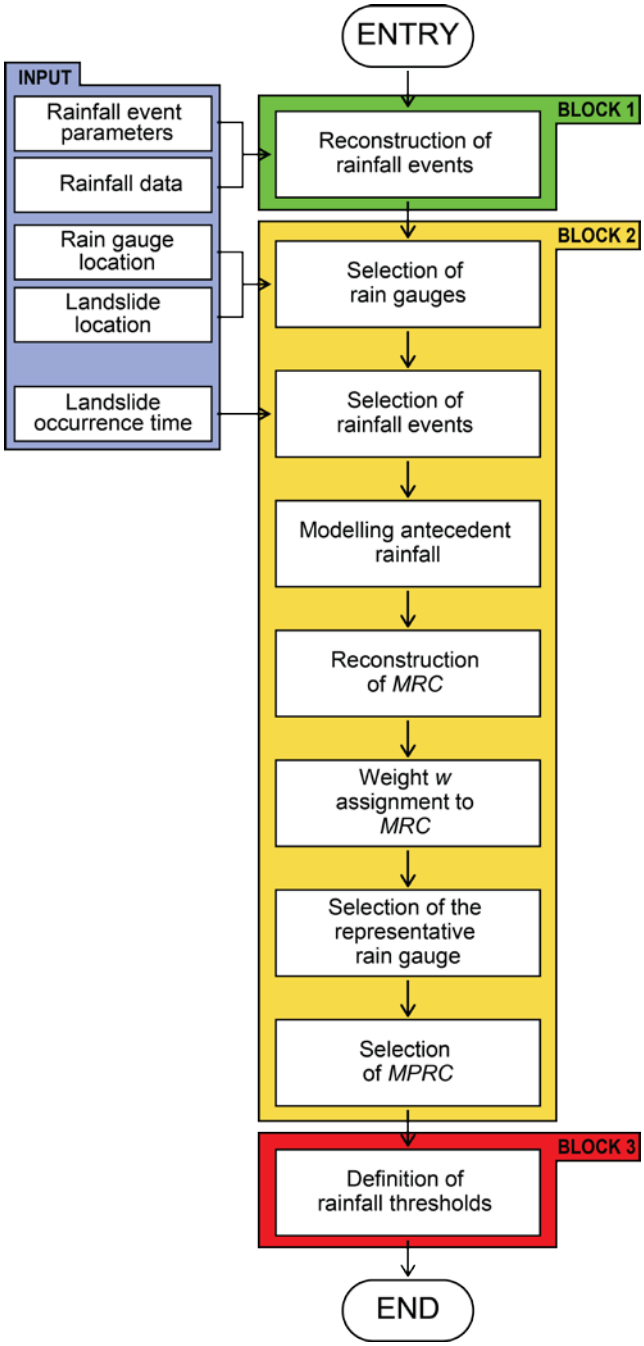

Figure 8. Logical framework of the algorithm in CTRL-T.

First, CTRL-T reconstructs individual rainfall events from a record of rainfall measurements. This is performed in five successive steps, including a pre-processing step. Figure 9 portrays the logical framework of “BLOCK 1”.

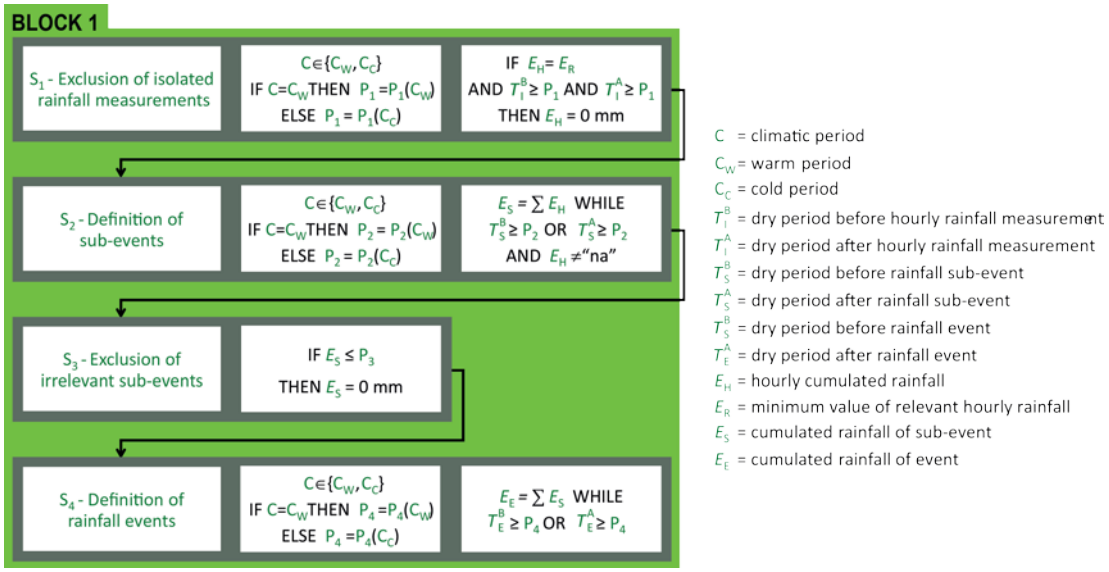

Figure 9. Logical framework of "BLOCK 1".

Step 0: Pre-processing of rainfall data

The tool works on a continuous (for the sake of the discussion, hourly) record of rainfall measurements obtained from a single rain gauge in a period. Records of rainfall measurements are typically discontinuous (incomplete), with individual or multiple rainfall measurements missing in the record due to technical and operational problems. The gaps in the record can cover periods ranging from a minimum of one hour to several days or weeks, and are typically marked by specific "tags" in the record, with different tags used to describe different types of technical and operational problems. Occasionally, tags are missing in the rainfall record, and it is difficult – or impossible – to single out measurements gaps in the record. The algorithm checks the continuity of the record and detects the gaps. More specifically, the algorithm searches the rainfall record for tagged and untagged missing measurements, and replaces them with the "na" tag (measurement not available).

In addition, a rainfall record may contain hourly rainfall measurements E_H that are lower than the instrumental sensitivity of a rain gauge (e.g., G_S = 0.2 mm), $E_H < G_S$. These hourly measurements are considered noise in the rainfall record, and the algorithm sets the measurements to E_H = 0.0 mm. Note that E_H = "na" is different from E_H = 0.0 mm. When E_H = "na" the rainfall information is missing in the record, whereas when E_H = 0.0 mm the rainfall information is available in the record and it is considered noise. Figure 10a shows a prototype example of a corrected rainfall record.

Step 1: Detection and exclusion of isolated rainfall measurements

The algorithm starts by searching for isolated hourly rainfall measurements in the corrected rainfall record (S_1 in Figure 9). An isolated rainfall measurement is defined as an hourly measurement separated from the immediately preceding and the immediately following rainfall measurements by dry periods (T_I^B before, and T_I^A after) that exceed a given length P_1. The length of the dry period (P_1) depends on the seasonal or the local climatic conditions C i.e., $P_1 = P_1(C)$.

In the Mediterranean region two seasonal periods can be identified for landslide initiation: (i) a "warm" spring-summer period C_W, and (ii) a "cold" autumn-winter period C_C. For the C_W warm period the dry interval separating isolated rainfall measurements is P_1 = 3 hours, and for the C_C cold period the dry interval is P_1 = 6 hours (Table 2). Once the isolated rainfall measurements are identified, their individual relevance for the reconstruction of the rainfall conditions responsible for possible landslide occurrence is evaluated. We consider relevant the isolated hourly rainfall measurements that exceed a minimum value E_R (e.g., E_R = 0.2 mm), $E_H > E_R$, and irrelevant the measurements with $E_H = E_R$. The later measurements, shown by red bars in Figure 10b, contribute a negligible (irrelevant) amount of rain to the rainfall event (e.g., due to the presence of fog and/or humidity in the air). For the purpose of the analysis, the algorithm sets the isolated, irrelevant measurements to E_H = 0.0 mm.

Step 2: Identification of rainfall sub-events

The algorithm proceeds by searching for individual rainfall sub-events (S_2 in Figure 9), where a rainfall sub-event is a period of continuous rainfall separated from the immediately preceding and the immediately following sub-events by dry periods with no rain. As before, the length P_2 of the dry period may vary, depending on the seasonal and the climatic conditions, $P_2 = P_2(C)$. The separation is justified by the observation that the meteorological conditions and the rainfall characteristics in the two climatic periods are different. In the C_W warm period, rainfall is primarily brought to the study area by local convective storms, whereas in the C_C cold period rainfall is most commonly the result of regional frontal systems. We acknowledge that this is a simplification, that convective storms can occur in the cold period, and that regional fronts can condition the rainfall regime in the warm period. In the two periods, rainfall events are reconstructed using a different set of parameters. As an example, in a Mediterranean climate, P_2 = 6 hours in the C_W warm period, and P_2 = 12 hours in the C_C cold period (Table 2). When reconstituting a rainfall sub-event, the algorithm checks for the continuity of the rainfall record in the sub-event. If single or multiple "na" measurements (interruptions) are found in the rainfall record in the period covered by the sub-event, the sub-event is excluded from the analysis. If no "na" measurements are found, the sub-event is defined (grey shaded areas in Figure 10c), and rainfall metrics are computed for the sub-event, including: (i) the sub-event duration DS, computed summing the number of hours in the sub-event, and (ii) the sub-event total rainfall E_S, computed by summing the hourly rainfall measurements in the sub-event, $E_S = \sum E_H$.

Step 3: Exclusion of irrelevant rainfall sub-events

Next, the algorithm searches for sub-events that can be considered irrelevant for the reconstruction of rainfall events responsible for landslide occurrence (S_3 in Figure 10). For the purpose, a sub-event is considered irrelevant if the cumulated (total) rainfall for the sub-event is lower than a given threshold value $E_S \leq P_3$, regardless of the duration of the sub-event. In a Mediterranean climate, P_3 = 1 mm (Table 2) is a reasonable threshold to exclude sub-events whose contribution can be considered irrelevant for the possible initiation of rainfall induced

landslides. Irrelevant sub-events (red bars in Figure 10d) are excluded from the subsequent analysis.

Step 4: Identification of rainfall events

In this step, the algorithm aggregates single or multiple sub-events to obtain single rainfall events (S_4 in Figure 9), where a rainfall event is a period of continuous rainfall, or an ensemble of periods of continuous rainfall, separated from the preceding and the successive events by dry periods. Again, the minimum length P_4 of the inter-event dry periods may vary, depending on meteorological and seasonal conditions i.e., $P_4 = P_4(C)$. As an example, to identify the rainfall events shown in Figure 9c, we used a minimum dry period P4 = 48 hours for the C_W warm period, and a minimum dry period of P4 = 96 hours for the C_C cold period (Table 2). Once all the events in the rainfall record are defined (green shaded areas in Figure 10e), the algorithm calculates rainfall metrics for each of the detected rainfall events, including: (i) the event duration D_E, computed summing the number of hours in the rainfall event (including hours for which $E_H = 0$), and (ii) the event total cumulated rainfall E_E, computed by summing the sub-event rainfall $E_E = \sum E_S$.

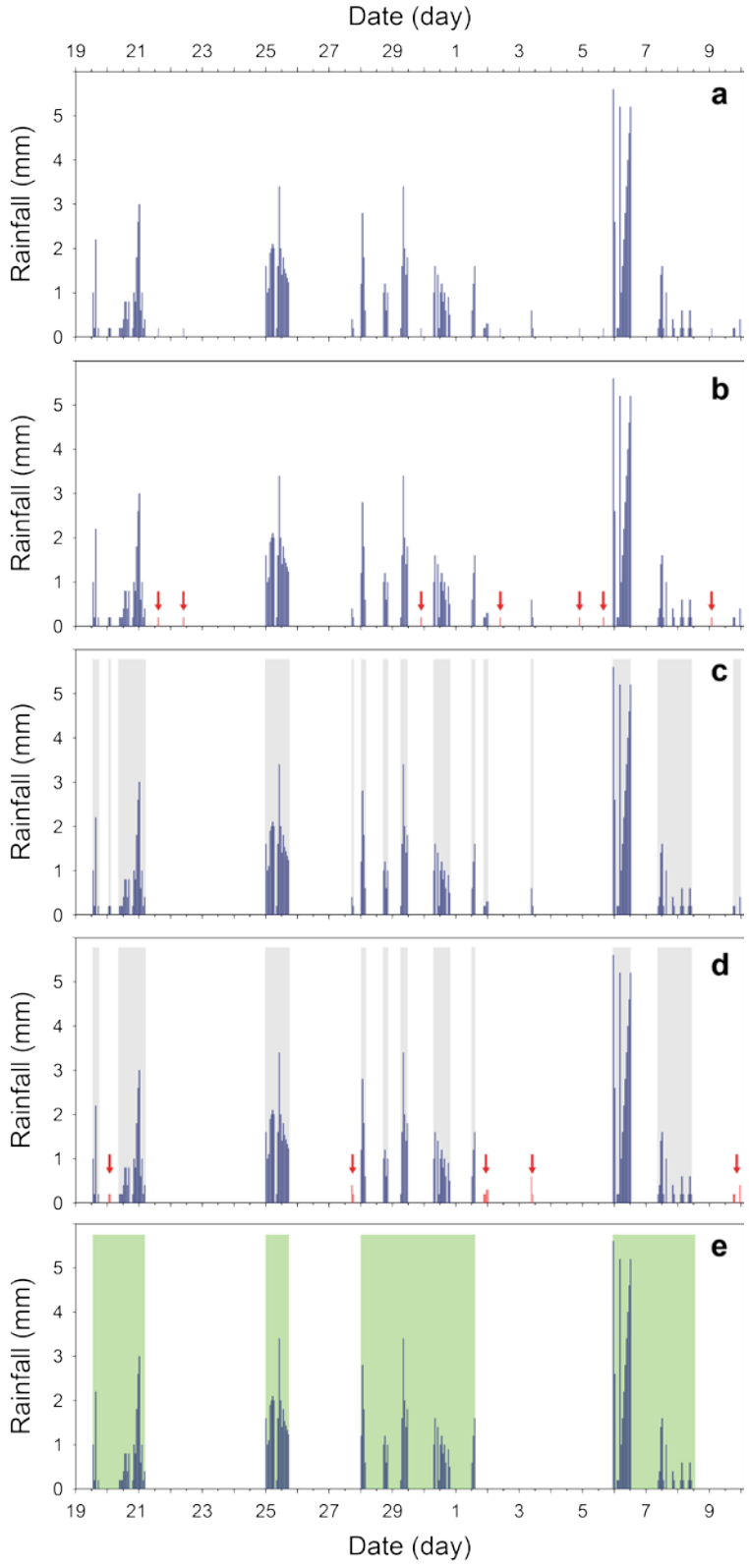

Figure 10. Example of the application of the tool for the reconstruction of rainfall events. (a) Blue bars show hourly rainfall measurements, from 19 September to 10 October 2006. (b) Selection of the isolated hourly rainfall measurements (red bars), shown by red arrows. (c) Identification of the rainfall sub-events, highlighted by grey-shaded areas. (d) Selection of irrelevant sub-events (red bars), shown by red arrows. (e) Identification of rainfall events, highlighted by green-shaded areas.

Table 2. Parameters used by CTRL-T in BLOCK 1. The first column lists the step in the logical framework of the algorithm where the parameter is used (see Figure 9). Two climatic periods are considered: C_W, a "warm" spring-summer period; and C_C, a "cold" autumn-winter period.

Step	Parameter name	Parameter value P(C_W)	Parameter value P(C_C)	Unit
S_0	G_S	2	2	mm
S_1	E_R	2	2	mm
S_1	P_1	3	6	h
S_2	P_2	6	12	h
S_3	P_3	1	1	mm
S_4	P_4	48	96	h

Using the information on the location of rain gauges and landslides provided by the "INPUT" section, "BLOCK 2" picks out the rain gauges closest to each landslide. CTRL-T selects automatically the representative rain gauge for a specific landslide from a pool of rain gauges located in a circular area (buffer) centred on the landslide location and with a parametrized radius (Rb, in Figure 11). Rb depends chiefly on the morphological settings of the study area and on the rain gauge density.

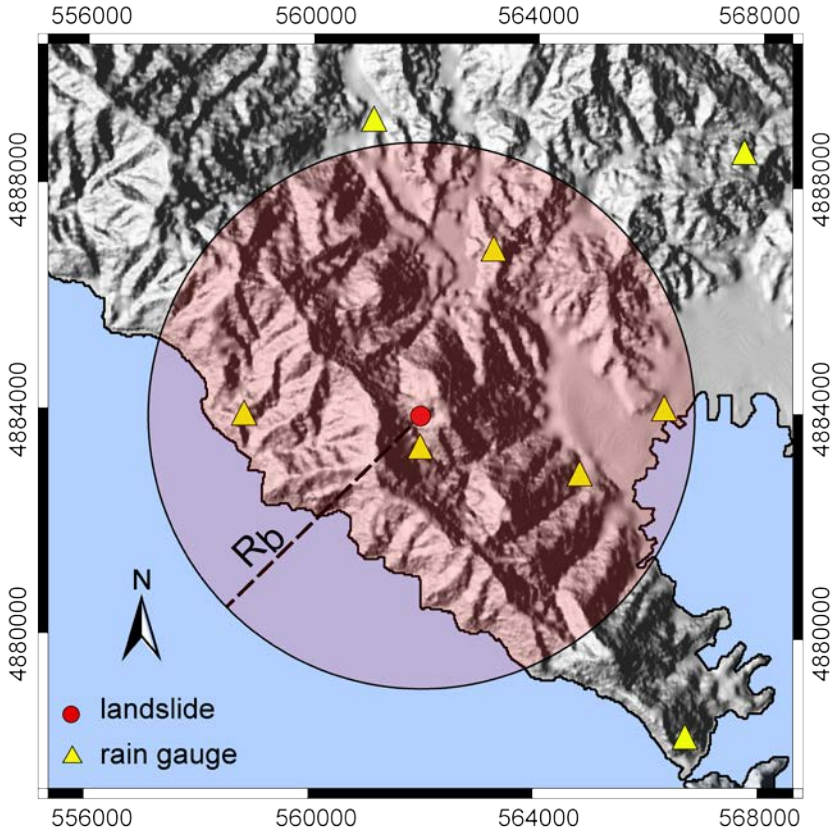

Figure 11. Selection of rain gauges (yellow triangles) in a circular buffer (red shaded area) centred in the landslide location (red dot) with a parametrized radius Rb (dashed black line).

For each selected rain gauge, CTRL-T identifies the rainfall event associated with the landslide. In particular, CTRL-T compares the dates (start date and end date) of the rainfall events identified by “BLOCK 1”, with a record listing the occurrence date (day and time) of the landslides. Each landslide in the temporal record is associated to a single rainfall event (Figure 12a). Next, CTRL-T calculates the rainfall metrics, D_L and E_L, responsible for the slope instability. Note that D_L and E_L responsible for landslide occurrence are not necessarily the same as the rainfall duration D_E and the cumulated event rainfall E_E of the rainfall event in Figure 12a. Most commonly, landslides occur before (and sometimes well before) the end of a rainfall period, and the rainfall after the landslide occurrence cannot be considered relevant for the initiation of the slope failure. In this case, $E_L \leq E_E$ and $D_L \leq D_E$. Occasionally, landslides fail after the end of the rainfall event. In this case, the cumulated rainfall responsible for the landslide corresponds to the cumulated event rainfall, $E_L = E_E$, and the rainfall duration is $D_L = D_E$. For complex rainfall events (Figure 12a) – which are the majority in a typical rainfall record – it is often difficult (or impossible) to decide a single duration, and the corresponding cumulated amount of rain responsible for the landslides. In this case, CTRL-T reconstructs multiple aggregations of rainfall sub-events that are likely to trigger landslides. In Figures 12b, 12c, 12d we show that the complex rainfall event portrayed in Figure 12a is characterized by three sub-events with significantly different rainfall durations (D_L = 28 h, 91 h, and 178 h) and cumulated rainfall amounts (E_L = 104.2 mm, 218.4 mm, and 263.2 mm). Without additional information, the three sub-events identified by the tool are equally probable as possible landslide triggers. Ultimately, CTRL-T identifies a variable number *n* of single (*n* = 1) or multiple rainfall conditions (MRC) likely responsible for each failure (e.g., 3 MRC for the example shown in Figure 11).

Through an empirical relation, that includes the distance between the rain gauge and the landslide, D_L and E_L, a weight *w* is assigned to each pair of the MRC data set.

$$w = \mathrm{f}(\mathrm{d}, E_L, D_L) = d^{-2} {E_L}^2 {D_L}^{-1} \quad (1)$$

The weight is attributed to each (D_L, E_L) pair of the MRC data set. For each landslide, *w* is used to identify the representative rain gauge, and to determine the probability of the single or multiple rainfall conditions to be adopted for the calculation of rainfall thresholds. For a pool of stations enclosed in the radius R_b, the representative rain gauge is the one for which the (D_L,E_L) pair has the highest *w*. In case of multiple pairs, each *w* is normalized to the sum of the individual weights, whereas is set to one in case of a single rainfall condition. The MRC corresponding to the maximum *w* (MPRC) is that likely responsible for the failure (red dot in Figure 12e).

In “BLOCK 3” CTRL-T calculates rainfall thresholds for MRC and MPRC (maximum probability rainfall conditions) data sets, where MPRC is the subset of the (D_L,E_L) pairs with the highest weights (Figure 13).

To define empirical rainfall thresholds and their associated uncertainties, CTRL-T adopts the frequentist statistical method proposed by Brunetti et al. (2010) and modified by Peruccacci et al. (2012) to calculate *ED* thresholds in Italy.

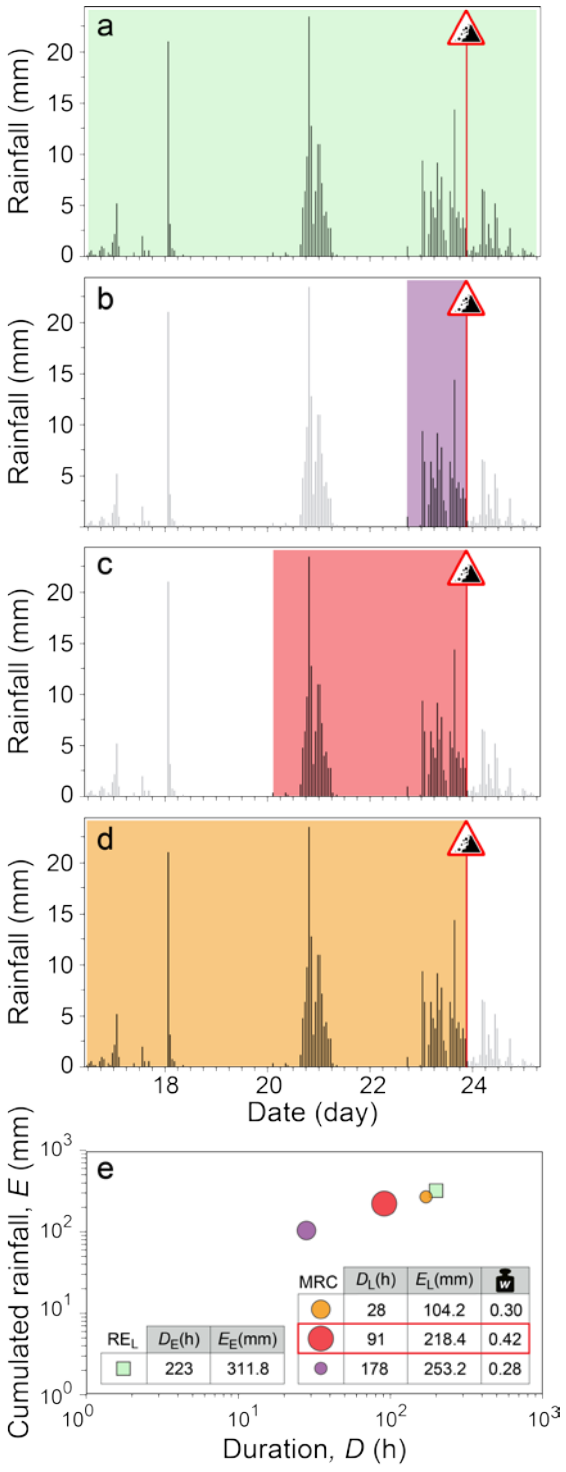

Figure 12. Example of the application of CTRL-T for the reconstruction of the rainfall conditions responsible for a failure. Traffic sign shows time of occurrence (23/12/2006, 10:00 PM), grey bars show hourly rainfall measurements. (a) Rainfall event identified by "BLOCK 1" containing a failure. (b) (c) (d) Multiple aggregations of rainfall sub-events with different values of D_L and E_L. (e). Green square shows the (D_E,E_E) pair of the rainfall event considered in (a). Purple, red, and orange dots show the (D_L,E_L) pairs of the rainfall conditions considered in (b), (c) and (d), respectively. The red rainfall condition is the most likely as trigger of the investigated landslide (MPRC).

The method avoids subjective criteria in the determination of the thresholds, which are common in many of the published rainfall thresholds for the possible initiation of landslides (Guzzetti et al. 2007, 2008). In particular, the method assumes in a Cartesian plane that the threshold curve is a power law of the form:

$$E = (\alpha \pm \Delta\alpha) \times D^{(\gamma \pm \Delta\gamma)} \quad (2)$$

where, E is the cumulated (total) event rainfall (in mm), D is the duration of the rainfall event (in h), α is a scaling parameter (the intercept), γ is the slope of the power law threshold curve, and $\Delta\alpha$ and $\Delta\gamma$ are the uncertainties associated to α and γ, respectively.

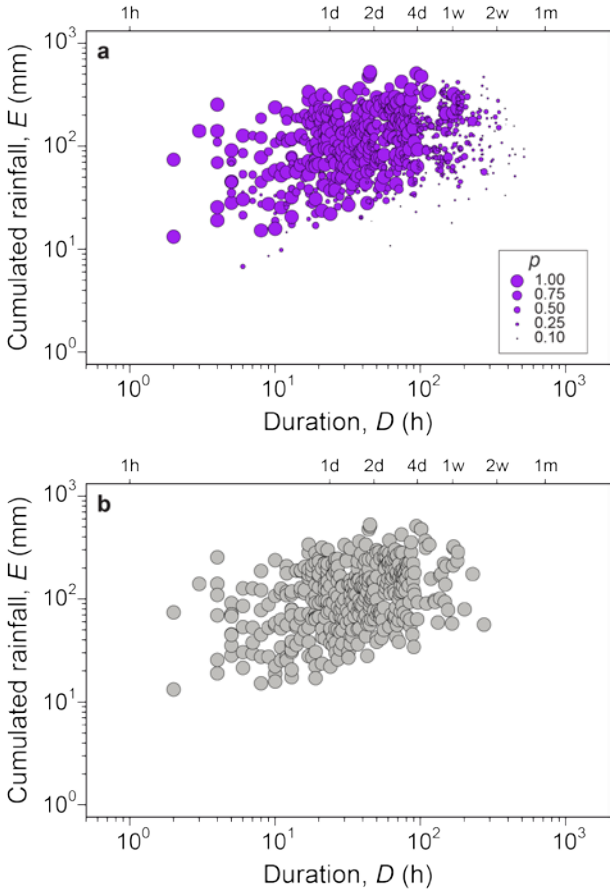

Figure 13. Example of the application of CTRL-T for the reconstruction of the rainfall conditions responsible for failures. Cumulated event rainfall E (mm) vs. rainfall duration D (h) conditions that have resulted in landslides using (a) the MRC and (b) the MPRC data set. In (a) frame, the size of the points (p probability) is proportional to the weight w of the (D_L,E_L) pairs.

Specifically, the ensemble of the (D,E) rainfall conditions responsible for the known slope failures is fitted with a power law. For each event, the difference between the cumulated event rainfall and the fit is calculated. The probability density of the distribution of the differences is determined through a Kernel Density approach, and the result modelled with a Gaussian function. Using the modelled distribution, thresholds corresponding to different non-exceedance probabilities are calculated (Brunetti et al. 2010). Assuming the set of the empirical (D_L,E_L) points is complete and

representative of the conditions that led to slope failures in a study area, the 1% threshold should leave 1% of the rainfall events with landslides below the curve.

A bootstrapping statistical technique is used to determine the uncertainty associated with the parameters α and γ that define the power law threshold curve (Peruccacci et al. 2012). In Eq. (2), α and γ are the mean values of the parameters resulting from the calculation of thresholds for 5000 synthetic series generated by the tool. $\Delta\alpha$ and $\Delta\gamma$ are the standard deviation of α and γ, respectively. Each synthetic series contains the same number n of landslides as the original data set but selected randomly with replacement (bootstrap technique). To calculate the thresholds, a single (D_L,E_L) pair is associated to each landslide. For each landslide in the individual synthetic series, the algorithm samples randomly − with a probability *w* − a single rainfall condition from the MRC data set. The extracted (D_L,E_L) pairs of the n landslide are used to define the thresholds. The algorithm also uses the rainfall conditions with the maximum w to define thresholds for the MPRC data set. The output of the bootstrapping technique consists of 5000 synthetic series of m (D_L,E_L) pairs. Analysis of the *m* synthetic series allows calculating the mean value and the uncertainty associated with the threshold parameters (α and γ) and their respective uncertainties ($\Delta\alpha$ and $\Delta\gamma$). The uncertainties associated with the model parameters decrease as the number of events increases and is also depending on the scatter of the (*D*,*E*) rainfall conditions around the fit. Figure 14 shows an example of *ED* power law thresholds (T_1, T_5, T_{10}, T_{20}, T_{35}, and T_{50}) corresponding to different exceedance probabilities (1%, 5%, 10%, 20%, 35% and 50%, respectively).

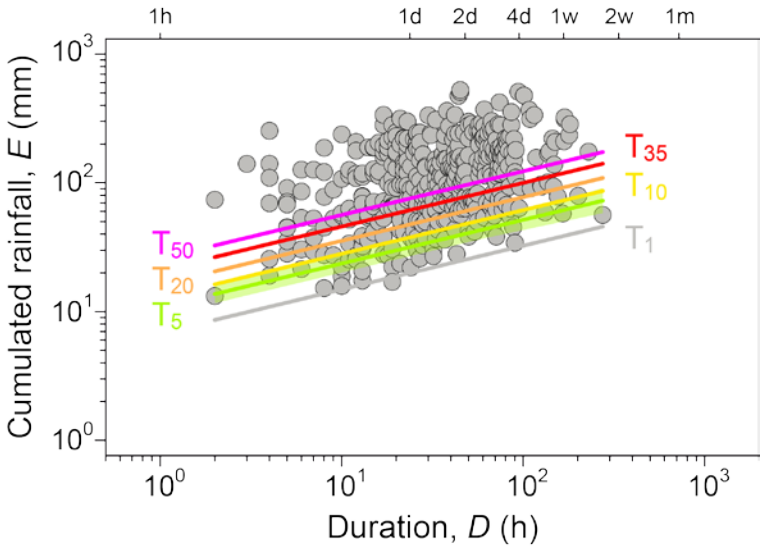

Figure 14. Example of ED rainfall thresholds at exceeding probabilities from 1% (T_1) to 50% (T_{50}) for the MPRC data set. Light grey dots are the (D_L,E_L) pairs. An example of the effect of the threshold uncertainty is shown for T_5 (light green shaded area).

Use of the algorithm accelerates greatly the compilation of large catalogues of rainfall events with landslides and reduces the uncertainty in the definition of landslide-triggering rainfall events.

5 RAINFALL THRESHOLDS

Using the catalogues of rainfall events with rockfalls presented before, and adopting the tool proposed by Melillo et al. (2018) we determined preliminary cumulated event rainfall–rainfall duration (ED) thresholds, and their associated uncertainties, for the Gran Canaria and Tenerife test sites. Table 3 lists the number of rainfall events with rockfalls used to define the thresholds, the equations of the power law curves used to represent each threshold, with their associated uncertainty, and the range of validity for the thresholds.

Table 3. Rainfall ED thresholds at different non-exceedance probabilities (1%, 5%, 10%, 20%, 35% and 50%) for the possible initiation of landslides in Gran Canaria e Tenerife test sites.

Threshold name	Number of rainfall conditions	Threshold equation	Duration range (h)
$T_{1,CAN}$	53	$E = (1.3\pm0.8)\times D^{(0.62\pm0.10)}$	24-264
$T_{5,CAN}$		$E = (2.0\pm1.2)\times D^{(0.62\pm0.10)}$	
$T_{10,CAN}$		$E = (2.4\pm1.5)\times D^{(0.62\pm0.10)}$	
$T_{20,CAN}$		$E = (3.2\pm2.0)\times D^{(0.62\pm0.10)}$	
$T_{35,CAN}$		$E = (4.1\pm2.7)\times D^{(0.62\pm0.10)}$	
$T_{50,CAN}$		$E = (5.2\pm3.4)\times D^{(0.62\pm0.10)}$	
$T_{1,TEN}$	230	$E = (1.0\pm0.2)\times D^{(0.76\pm0.05)}$	24-360
$T_{5,TEN}$		$E = (1.5\pm0.3)\times D^{(0.76\pm0.05)}$	
$T_{10,TEN}$		$E = (1.8\pm0.3)\times D^{(0.76\pm0.05)}$	
$T_{20,TEN}$		$E = (2.2\pm0.4)\times D^{(0.76\pm0.05))}$	
$T_{35,TEN}$		$E = (2.7\pm0.5)\times D^{(0.76\pm0.05)}$	
$T_{50,TEN}$		$E = (3.3\pm0.6)\times D^{(0.76\pm0.05)}$	

Figure 15 shows, in logarithmic coordinates, the distribution of the (*D*,*E*) rainfall conditions that have caused landslides in Gran Canaria (53 blue dots). In the log-log plot, the blue curve is the preliminary 5% *ED* threshold for the Gran Canaria test site ($T_{5,CAN}$). In Figure 16, the same threshold is shown in linear coordinates and in the range $24 \leq D \leq 120$ h, a typical range of rainfall duration used to forecast rainfall-induced landslide. The uncertainty associated with the threshold (blue shaded area in the Figure 16) is large due to the limited number of (*D,E*) rainfall conditions.

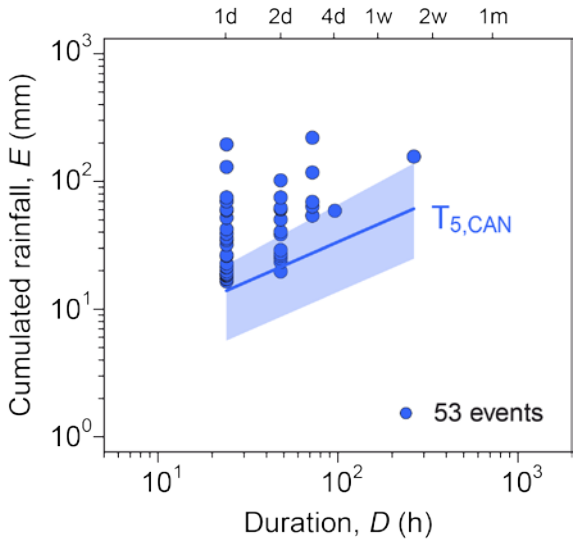

Figure 15. Rainfall duration D (x-axis) and cumulated event rainfall E (y-axis) conditions that have produced landslides in Gran Canaria test site (53 blue dots). Blue curve is 5% power law thresholds ($T_{5,CAN}$). Shaded area show uncertainty associated with the threshold curve. Data shown in logarithmic coordinates.

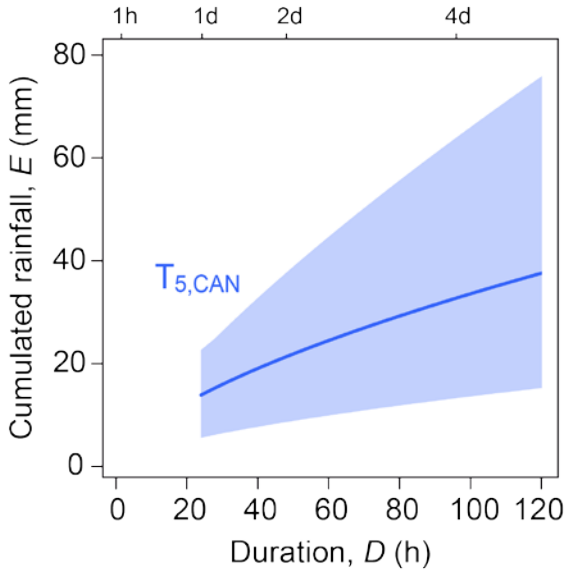

Figure 16. 5% ED threshold for Gran Canaria test site ($T_{5,CAN}$) in linear coordinates, in the range of durations 24 ≤ D ≤ 120 h. Shaded areas show uncertainty associated with the threshold curve.

Coloured curves in Figure 17 are the preliminary *ED* power law thresholds ($T_{1,CAN}$, $T_{5,CAN}$, $T_{10,CAN}$, $T_{20,CAN}$, $T_{35,CAN}$, and $T_{50,CAN}$) corresponding to different non-exceedance probabilities (1%, 5%, 20%, 35% and 50%, respectively) for Gran Canaria test site (Table 3).

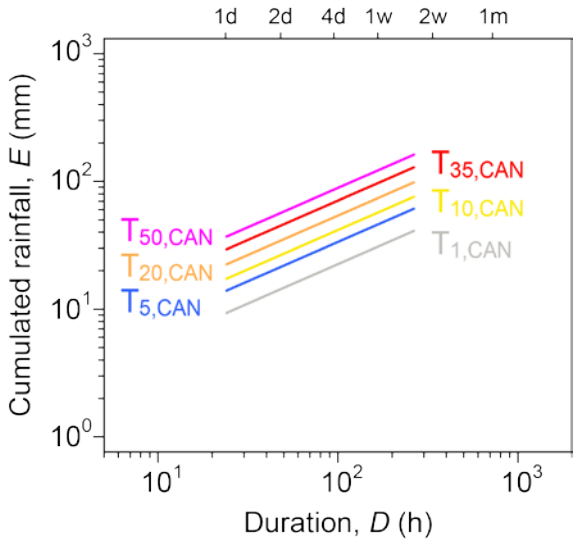

Figure 17. ED rainfall thresholds at 1%, 5%, 10%, 20%, 35% and 50% non-exceeding probabilities ($T_{1,CAN}$, $T_{5,CAN}$, $T_{10,CAN}$, $T_{20,CAN}$, $T_{35,CAN}$ and $T_{50,CAN}$) for Gran Canaria test site. Data shown in logarithmic coordinates.

Figure 18 shows, in logarithmic coordinates, the distribution of the (*D*,*E*) rainfall conditions that have caused landslides in Tenerife (230 green dots). In the log-log plot, the green curve is the preliminary 5% *ED* threshold for the Tenerife test site ($T_{5,TEN}$).

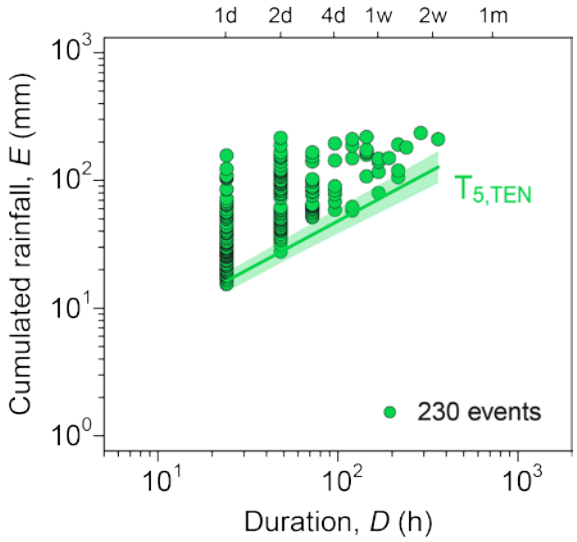

Figure 18. Rainfall duration D (x-axis) and cumulated event rainfall E (y-axis) conditions that have produced landslides in Tenerife test site (230 green dots). Green curve is 5% power law thresholds ($T_{5,TEN}$). Shaded area show uncertainty associated with the threshold curve. Data shown in logarithmic coordinates.

In Figure 19, the same threshold is shown in linear coordinates and in the range $24 \leq D \leq 120$ h, a typical range of rainfall duration used to forecast rainfall-induced landslide.

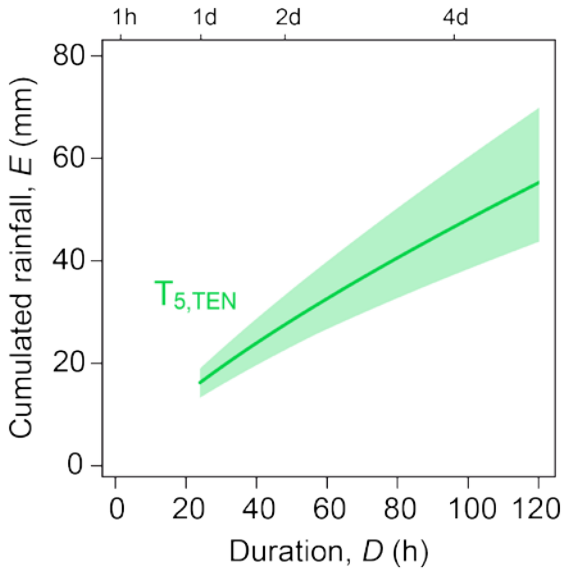

Figure 19. 5% ED threshold for Tenerife test site ($T_{5,TEN}$) in linear coordinates, in the range of durations 24 ≤ D ≤ 120 h. Shaded areas show uncertainty associated with the threshold curve.

Coloured curves in Figure 20 are the preliminary *ED* power law thresholds ($T_{1,TEN}$, $T_{5,TEN}$, $T_{10,TEN}$, $T_{20,TEN}$, $T_{35,TEN}$, and $T_{50,TEN}$) corresponding to different non-exceedance probabilities (1%, 5%, 20%, 35% and 50%, respectively) for Tenerife test site (Table 3).

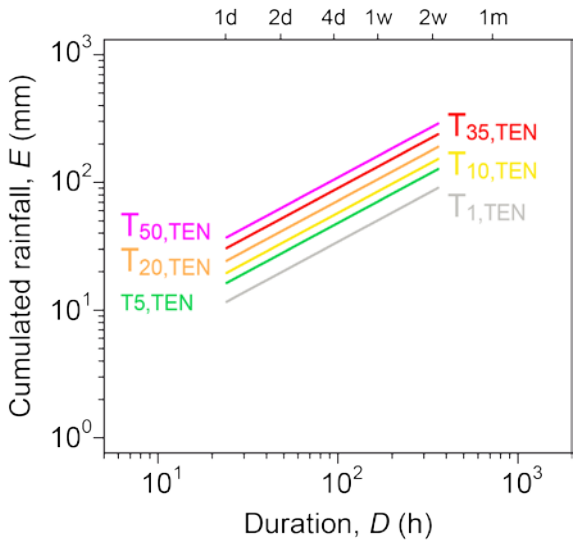

Figure 20. ED rainfall thresholds at 1%, 5%, 10%, 20%, 35% and 50% non-exceeding probabilities ($T_{1,TEN}$, $T_{5,TEN}$, $T_{10,TEN}$, $T_{20,TEN}$, $T_{35,TEN}$ and $T_{50,TEN}$) for Tenerife test site. Data shown in logarithmic coordinates.

Figure 21 portrays $T_{5,CAN}$ (blue curve) and $T_{5,TEN}$ (green curve) in logarithmic coordinates, with the shaded area showing the uncertainty associated with the thresholds. Inspection of the figure reveals that $T_{5,CAN}$ and $T_{5,TEN}$ are similar. Further inspection indicates that $T_{5,TEN}$ is slightly steeper and higher than $T_{5,CAN}$. This could mean that, increasing rainfall duration, a smaller amount of

rainfall is necessary to trigger landslides in the Gran Canaria test site, rather than in the Tenerife test site. The trend for each test site has to be confirmed by collecting a larger number of events.

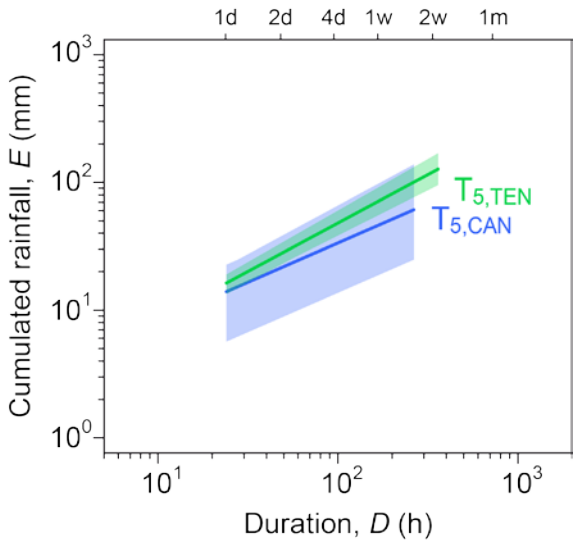

Figure 21. Comparison between the 5% ED thresholds for Gran Canaria ($T_{5,CAN}$) and for Tenerife ($T_{5,TEN}$) test sites. Data shown in logarithmic coordinates.

The obtained thresholds for different exceedance probabilities are suited for the design of probabilistic schemes for the prediction of rainfall-induced landslides in early warning systems.

REFERENCES

Aleotti P (2004). A warning system for rainfall-induced shallow failures. Eng. Geol. 73, 247–265. https://doi.org/10.1016/j.enggeo.2004.01.007.

Berti M, Martina MLV, Franceschini S, Pignone S, Simoni A, Pizziolo M (2012). Probabilistic rainfall thresholds for landslide occurrence using a Bayesian approach. J. Geophys. Res. 117, F04006, https://doi.org/10.1029/2012JF002367.

Brunetti MT, Peruccacci S, Rossi M, Luciani S, Valigi D, Guzzetti F (2010). Rainfall thresholds for the possible occurrence of landslides in Italy. Nat Hazards Earth Syst Sci 10, 447–458. https://doi.org/10.5194/nhess-10-447-2010

Campbell RH (1975). Soil slips, debris flows, and rainstorms in Santa Monica Mountains and vicinity, Southern California. US Geol. Survey, Prof. Paper 851, 55pp. https://pubs.usgs.gov/pp/0851/report.pdf

Giannecchini R, Galanti Y, D'Amato Avanzi G (2012). Critical rainfall thresholds for triggering shallow landslides in the Serchio River Valley (Tuscany, Italy). Nat. Hazards Earth Syst. Sci. 12, 829-842. https://doi.org/10.5194/nhess-12-829-2012.

Guzzetti F, Peruccacci S, Rossi M, Stark CP (2007). Rainfall thresholds for the initiation of landslides in central and southern Europe. Meteorol. Atmos. Phys. 98 (3), 239–267. https://doi.org/10.1007/s00703-007-0262-7.

Guzzetti F, Peruccacci S, Rossi M, Stark CP (2008). The rainfall intensity–duration control of shallow landslides and debris flows: an update. Landslides 5 (1), 3–17. https://doi.org/10.1007/s10346-007-0112-1.

Martelloni G, Segoni S, Fanti R, Catani F (2012). Rainfall thresholds for the forecasting of landslide occurrence at regional scale. Landslides 9, 485-495. https://doi.org/10.1007/s10346-011-0308-2.

Melillo M, Brunetti MT, Peruccacci S, Gariano SL, Roccati A, Guzzetti F (2018). A tool for the automatic calculation of rainfall thresholds for landslide occurrence. Environmental Modelling & Software, 105, 230-243. https://doi.org/10.1016/j.envsoft.2018.03.024

Peruccacci S, Brunetti MT, Luciani S, Vennari C, Guzzetti F (2012). Lithological and seasonal control of rainfall thresholds for the possible initiation of landslides in central Italy. Geomorphology, 139-140, 79–90. https://doi.org/10.1016/j.geomorph.2011.10.005.

Peruccacci S, Brunetti MT, Gariano SL, Melillo M, Rossi M, Guzzetti F (2017). Rainfall thresholds for possible landslide occurrence in Italy. Geomorphology, 290, 39–57. https://doi.org/10.1016/j.geomorph.2017.03.031.

Rosi A, Peternel T, Jemec-Auflič M, Komac M, Segoni S, Casagli N (2016). Rainfall thresholds for rainfall-induced landslides in Slovenia. Landslides 13, 1571–1577. https://doi.org/10.1007/s10346-016-0733-3.

Segoni S, Rossi G, Rosi A, Catani F (2014). Landslides triggered by rainfall: a semi-automated procedure to define consistent intensity–duration thresholds. Comput. Geosci., 63, 123-131, 10.1016/j.cageo.2013.10.009.
https://www.sciencedirect.com/science/article/pii/S0098300413002732?via%3Dihub

Staley DM, Kean JW, Cannon SH, Schmidt KM, Laber JL (2013). Objective definition of rainfall intensity–duration thresholds for the initiation of post-fire debris flows in southern California. Landslides 10, 547-562. https://doi.org/10.1007/s10346-012-0341-9.

Wieczorek GF (1987). Effect of rainfall intensity and duration on debris flows in central Santa Cruz Mountains. In: Costa JE, Wieczorek GF (Eds.), Debris flow-avalanches: process, recognition, and mitigation. Geological Society of America, Reviews Eng. Geol. 7, 93-104.

Wilson RC (2000). Climatic variations in rainfall thresholds for debris-flows activity. In: Claps P, Siccardi F (Eds.) Proceedings 1st EGS Plinius Conference on Mediterranean Storms, Maratea, 415-424.